RF GUN FOR ILU-12 ACCELERATOR

V.L. Auslender, I.V. Gornakov, G.I. Kuznetsov, I.G. Makarov, N.V. Matyash, G.N. Ostreiko, A.D. Panfilov, G.V. Serdobintsev, V.V. Tarnetsky, M.A. Tiunov
Budker INP SB RAS, Novosibirsk, Russia
E-mail: M.A.Tiunov@inp.nsk.su, Phone: +7(383)339-45-54

RF gun for ILU-12 accelerator is described in the paper. Mechanism of beam transportation and energy spectrum improvements by applying an additional RF voltage of the operating frequency to the cathode-grid gap is considered in detail. Simulated energy spectrum and density profile of electron beam at the accelerator output are presented.

PACS: 29.17.+w, 29.27.-a, 29.27.Ac

1. INTRODUCTION

High power RF accelerator prototype for industrial applications, named ILU-12, was developed, manufactured and now successfully started up in Budker INP, Novosibirsk [1-2]. Main parameters of the accelerator are: operating frequency of 176 MHz, energy of electrons of 5 MeV, pulse beam power up to 2 MW. General view of the accelerator is shown on Fig.1.

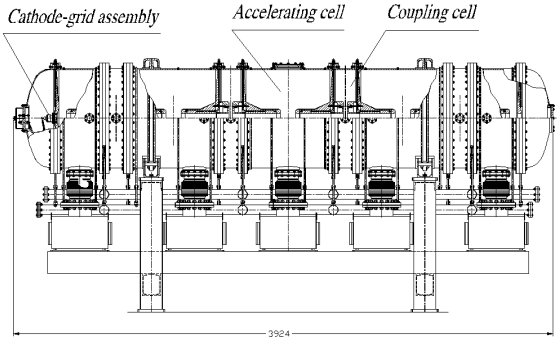

Fig.1. General view of ILU-12 accelerator

The electrons are accelerated in the multi-resonator standing wave structure with on-axis coupling resonators. Such design makes it possible to decrease power losses in each resonator comparing to the single-resonator accelerator (at the same average beam power level) and to obtain the electron efficiency of the accelerating structure of about 70%.

The internal beam injection from the cathode-grid assembly, which is placed directly to the first accelerating gap, is used. This concept permits us to sufficiently simplify the design and reduce the cost of the accelerator respectively, as well as to improve its reliability and reduce the maintenance charges.

Two important tasks may be emphasized from a quantity of problems that must be solved for accelerator prototype successful start up:

- achievement of the required value of the pulse beam current at relatively low electric field strength in the accelerating gaps comparing with the single-resonator accelerator;
- lossless transportation of a powerful electron beam through the accelerating structure without usage of electro- and magnetostatic lenses.

To solve these problems, a new cathode-grid assembly was designed. General view of this important component is shown on Fig.2 [3]. To optimize the injection of current together with longitudinal beam dynamics the additional RF bias voltage of operating frequency is used.

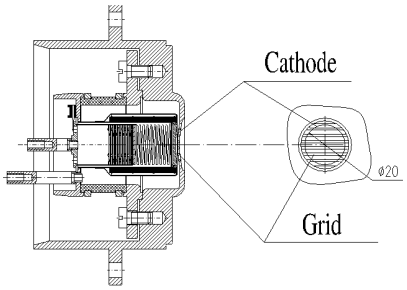

Fig.2. General view of cathode-grid assembly

The report describes results of detailed simulation of internal injection and beam dynamics in ILU-12 accelerator. Computer simulations were performed in long-wave approximation using ExtraSAM [4] and SAM [6] codes, modified for solution of the problems mentioned above. Simulated beam profile and energy spectrum at the accelerator output are presented.

2. INTERNAL INJECTION SIMULATION

2.1. 2D MODEL OF THE CATHODE-GRID ASSEMBLY CELL

Figure 3 presents the cathode-grid assembly model for 2D simulation. The main geometric parameters of the assembly are: the cathode-grid gap *d*, step of the grid *h*, and diameter of wires *D*.

The computer optimization of these parameters was carried out with ExtraSAM program package [5] modified for time-dependent modeling of the effect of emission limitation by the beam space charge. All the cathode-grid assembly simulation results presented below were obtained using the following optimized geometric parameters: d = 1.5 mm, h = 3 mm, D = 1 mm.

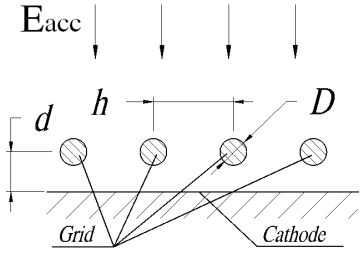

Fig.3. 2D model of the cathode-grid assembly

To optimize the injection of current together with longitudinal beam dynamics the additional RF bias voltage of operating frequency is used. The control cathode-grid voltage has the following time dependence:

$$U_g(t) = U_0 + U_1 \sin(\omega t + \phi_1), \quad (1)$$

here U_0 is the constant bias voltage on the cathode-grid assembly, U_1 and φ_1 are amplitude and phase shift of the additional bias RF voltage at operating frequency, $\omega t=2\pi \cdot f \cdot t$ – phase of the accelerating field. The simulations were performed for the amplitude of the accelerating field at the grid plane E_{acc}=85 kV/cm (see Fig.3) in phase range from 0˚ to 140˚ with maximal number of phase layers of particles $N\varphi$=140. All presented below results are obtained using the following optimized parameters: U_0=-2,1kV, U_1=2kV, φ_1=60°.

Fig.4 shows the simulation results for a single cell of the cathode-grid assembly.

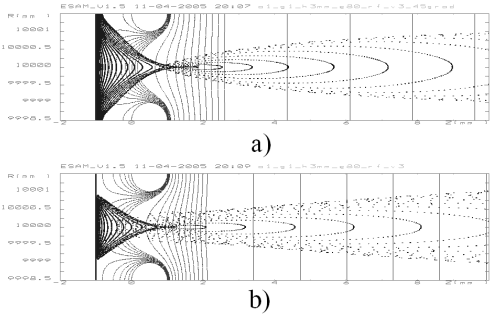

Fig.4. Results of time-dependent modeling of single cell of the cathode-grid assembly: a) maximum cathode current at the accelerating field phase of 45°; b) half of maximum cathode current at phase of 70° (lines – equipotential lines, points – phase layers of particles)

2.2. 3D MODEL OF THE CATHODE-GRID ASSEMBLY

A simulation 3D model of the cathode-grid assembly (see Fig.5) was developed to describe the beam injection into the accelerator. It considers existence of seven various-length longitudinal slots in the grid located in front of the 20 mm cathode. Besides, the spherical form of the grid and cathode is also taken into account.

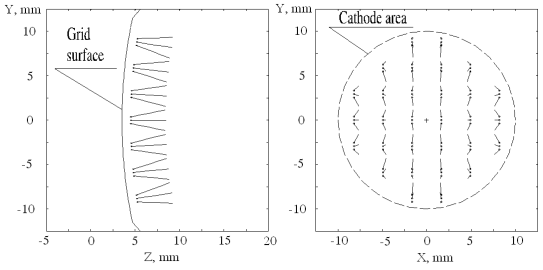

a) *b)*

Fig.5. 3D model of the cathode-grid assembly for Nx=6 and Ny=3: a) YZ projection; b) XY projection

The beam time-dependent flow characteristics from a single cathode-grid assembly cell at 1 mm distance from the grid surface were used for calculation of the macro particles starting parameters in 3D beam dynamics simulation. Here, the cathode start transverse coordinates for each slot was defined equidistantly, a total of *Ny* points.

To describe the beam parameters along slots, the slots were divided into equal micro cells, at that their maximal number *Nx* was defined for the central slot. Length of each cell was determined by condition that the micro cell central point did not leave the cathode area.

3. BEAM DYNAMICS SIMULATION

3.1. CALCULATION OF CURRENT MICRO PULSE AND BEAM SPECTRUM

Calculation of the macro particle dynamics in the accelerator starts at a distance of 1 mm behind the grid. Here, the transit effect leads to delay in electron departure from the cathode-grid assembly and deformation of the current micro pulse form.

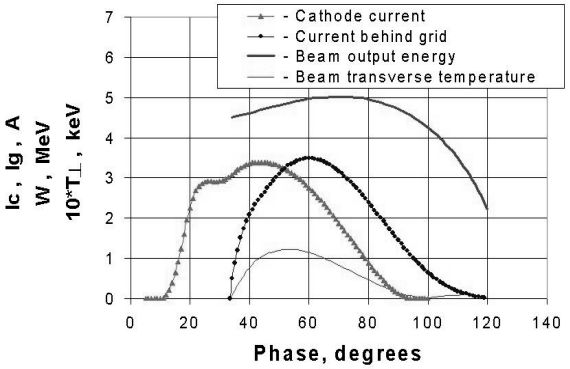

Fig.6. Accelerating field on the cathode phase dependencies of the current micro pulse and beam output parameters

So, by time-dependent code together with calculation of current micro pulse form at the cathode, the calculation of the current micro pulse form behind the grid was carried out. On Fig.6 the curves with triangles and circles show the simulation results for current micro pulse form on the cathode and at a distance of 1 mm behind the grid respectively.

3D beam dynamics simulation in the accelerator was carried out by modified SAM code [5] with long-wave approximation of fields and taking into account the form of micro pulse of current behind the grid. Simulation results for the accelerating field phase dependencies of the beam energy and effective transverse temperature at the accelerator output are also presented in Fig.6.

As may be seen from Fig.6, the electron output energy substantially depends on the accelerating field phase on the cathode. Just this fact leads to necessity of the use of an additional first harmonic voltage at the cathode-grid gap to shift the current micro pulse into the acceptable phase area and narrowing the beam energy spectrum. As a result, a mean square electron energy deviation from the beam average energy 4,83 MeV amounts to only 3,3%.

Beneficial effect of an additional first harmonic using was experimentally proven at the present single-gap accelerator ILU-10 [6].

3.2. BEAM TRANSPORTATION THROUGH THE ACCELERATOR

The calculated pulse output power of the beam with parameters presented in Fig.6 is equal to 2,15 MW. For such high-power beam the problem of lossless transportation becomes very important. Here, it is necessary to keep in mind the space charge influence on the elec-

tron transverse dynamics, especially at the first acceleration stage. So, for every macro particle the effective beam space charge transverse field was calculated:

$$E_r^{(q)} = \frac{Z_0 \cdot J(t) \cdot r_0^2}{2 \cdot \pi \cdot r \cdot \beta \cdot \gamma^2}, \qquad (2)$$

here $Z_0 \approx 120 \cdot \pi \ (\Omega)$ is the impedance of free space, $J(t)$ is the dynamic value of the average emission current density for a macro particle with starting time t, calculated by time-dependent code; r_0 is the macro particle starting radius; r, β and γ are the current values of macro particle radius, relative velocity and relativistic factor.

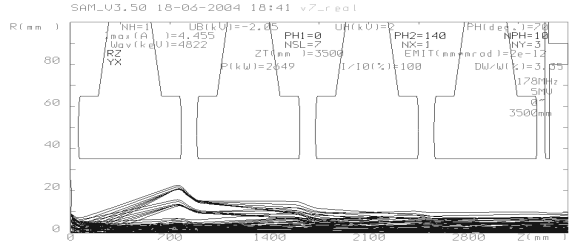

Fig.7. Typical view of electron trajectories in the accelerator

Fig.7 presents a typical view of electron trajectories in the accelerator (*Nx*=1, *Ny*=3, *Nφ*=10). As is obvious from the figure, the beam consists of the central core formed by electrons started from centers of slots in the grid and moved transversely to the cathode. Also there is a noticeable halo formed by electrons started from edges of slots and moved at some angle to the normal. The results presented were obtained after optimization of the cathode-grid assembly sphere radius of curvature and accelerator aperture. Simulations proved the possibility to transport the beam through the accelerator at the expense of aperture increasing up to 70 mm and RF focusing effect without using additional focusing elements.

Fig.8 presents the calculated profiles (Nx=30, Ny=19, Nφ=70) of an average beam current density in the micropulse at the second accelerating gap input (a), in the middle between the third and fourth gaps (b), at the accelerator output (c), and at a distance of 1,5 m from the accelerator output (d). Beam transverse dimensions are shown in millimeters.

Due to injection transverse velocity spread only across the slots, the beam current density profile has an elliptical shape at the second accelerating gap entrance (see Fig.8,a). During beam accelerating RF focusing leads to progressive elimination of this effect in the middle between the third and fourth gaps (Fig.8,b), and at the accelerator output (Fig.8,c). However, in this case the overfocusing of extreme particles takes place, and the beam profile obtains slightly elliptical shape again at a distance of 1,5 m from the accelerator (Fig.8,d). This effect may be eliminated through additional beam magnetic focusing in beam deflecting device at the target.

The results of first experiments on ILU-12 accelerator [3] are in good agreement with simulation results. With use additional RF voltage on the cathode it is possible to transport through accelerating structure 95% of current of 1,5 MW pulse power electron beam. Also the energy spectrum of electron beam at the accelerator output is improved.

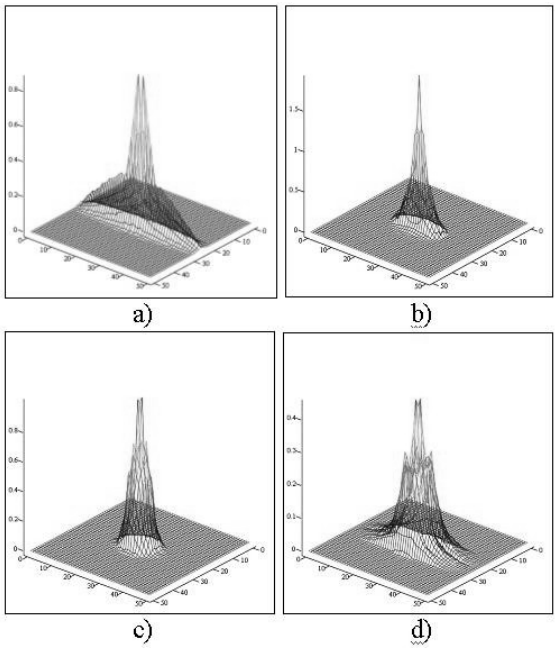

Fig.8. Profiles of an average beam current density at the different stages of accelerating

CONCLUSION

The results obtained proved the possibility to achieve the required value of the pulse beam current and to transport a powerful electron beam through the accelerating structure without usage of electro- and magnetostatic lenses. It became possible by using the internal beam injection from specially designed cathode-grid assembly with applying a constant biasing voltage and an additional bias RF voltage of operating frequency with appropriate phase shift.

The results of first experiments on ILU-12 accelerator are in good agreement with simulation results.

This work is supported by DOE, ISTC Project #2550.

REFERENCES

1. M. Tiunov, et al. // *Proceedings of EPAC 2002, Paris, Franc.,* 2002, p.2813-2815.
2. V.L. Auslender, et al. // *Proceedings of PAC 2005, Knoxville, USA*. 2005, p.1502-1504.
3. M.A. Tiunov, et al. // Nuclear Instruments and Methods. 2006, v.A558, p.77-84.
4. M. Tiunov, G. Kuznetsov, M. Batazova *// AIP Conference Proceedings*. 2001, v.572, №1, p.155-164.
5. B. Fomel, M. Tiunov, V. Yakovlev // *Preprint Budker INP 96-11*. 1996.
6. V.L. Auslender, et al. // *Proceedings of the RuPAC 2004, Dubna, JINR*. 2005, p.116-120.

ВЫСОКОЧАСТОТНАЯ ПУШКА УСКОРИТЕЛЯ ИЛУ-12

В.Л. Ауслендер, И.В. Горнаков, Г.И. Кузнецов, И.Г. Макаров, Н.В. Матяш, Г.Н. Острейко, А.Д. Панфилов, Г.В. Сердобинцев, В.В. Тарнецкий, М.А. Тиунов

Дается описание ВЧ-пушки ускорителя ИЛУ-12. Детально рассматривается механизм улучшения прохождения пучка и его энергетического спектра путем подачи дополнительного ВЧ-напряжения рабочей частоты на зазор сетка-катод. Приводятся расчетные спектр энергии и профиль плотности электронного пучка на выходе ускорителя.

ВИСОКОЧАСТОТНА ГАРМАТА ПРИСКОРЮВАЧА ІЛУ-12

В.Л. Ауслендер, І.В. Горнаков, Г.І. Кузнецов, І.Г. Макаров, Н.В. Матяш, Г.Н. Острейко, А.Д. Панфілов, Г.В. Сердобінцев, В.В. Тарнецький, М.А. Тіунов

Дається опис ВЧ-гармати прискорювача ІЛУ-12. Детально розглядається механізм поліпшення проходження пучку і його енергетичного спектра шляхом подачі додаткової ВЧ-напруги робочої частоти на зазор сітка-катод. Приводяться розрахункові спектр енергії і профіль щільності електронного пучку на виході прискорювача.